FOREX Publication
Open Access | Rapid and quality publishing
International Journal of Electrical and Electronics Research (IJEER)
Research Article | Volume 13, Issue 2 | Pages 193-198 | e-ISSN: 2347-470X

Extending the Hopf Bifurcation Limit Using Power System Stabilizer in a Two Area Power System Having Huge Industrial Loads

Ghousul Azam Shaik[1*], and Lakshmi Devi Aithepalli[2]
[1]*Department of Electrical and Electronics Engineering, SVU College of Engineering, Sri Venkateswara University, Tirupati – 517 502, India; ghousul1993@gmail.com*
[2]*Department of Electrical and Electronics Engineering, SVU College of Engineering, Sri Venkateswara University, Tirupati – 517 502, India; energylak123@yahoo.comsatish_8020@yahoo.co.in*

***Correspondence:** *ghousul1993@gmail.com*

ABSTRACT- The phenomenon of Hopf bifurcation is observed in several engineering and non-engineering domains which use both linear and nonlinear dynamic models. One parameter and two parameter variations of set of Differential Algebraic Equations of Kundur two area system was explored in this manuscript assisted with eight different cases to have detailed insight into Hopf bifurcation by modelling the load buses with industrial loads. The effect of PSS on improving the damping ratio and increase in the maximum loading at the industrial load buses was showcased by taking Hopf bifurcation as a tool for assessing the same by increasing the generation.

Keywords: Damping ratios, Hopf bifurcation point, Inter-area mode, Power System Stabilizer.

ARTICLE INFORMATION
Author(s): Ghousul Azam Shaik, Lakshmi Devi Aithepalli;
Received: 20/11/2024; **Accepted**: 03/04/2025; **Published**: 25/04/2025;
e-ISSN: 2347-470X;
Paper Id: IJEER 2011-19;
Citation: 10.37391/ijeer.130202
Webpage-link:
https://ijeer.forexjournal.co.in/archive/volume-13/ijeer-130202.html

crossref member
CROSSREF.ORG THE CITATION LINKING BACKBONE

Publisher's Note: FOREX Publication stays neutral with regard to Jurisdictional claims in Published maps and institutional affiliations.

1. INTRODUCTION

The demand for electricity is increasing since the starting of industrial revolution. The operators of the utilities need to have an eye on the maximum allowable capacity that load can be handled via increase in generation. In this manuscript, the Hopf bifurcation concept is used to see how much the load demand at a particular PQ load node can be met. Power System Stabilizers (PSS) can be installed to improve the overall small signal stability along with Automatic Voltage Regulator (AVR) to improve the damping torque. A comprehensive knowledge regarding the types and various models of PSS to improve low frequency oscillations was given by [1]. In order to solve the system algebraic equations, some numerical methods needed are given in [2].

Extensive methods on well-conditioned and ill conditioned methods to find the network solutions by considering constant power type of load is mentioned in [2]. It gave details of Newton and non-Newton based application methods to power system problems. Improving small signal stability in renewable integrated power network using PSS designed by using salp swarm optimization technique by considering IEEE DC exciter attached to each generator details are given by [3]. In [3], loads are modelled by constant power (CP). They didn't consider the performance of PSS near Hopf bifurcation point. Authors of this manuscript chose to use static exciter and ZIP industrial load model. The phenomenon on Hopf bifurcation in Western States Coordinating Council (WSCC) system to see the maximum loadability at a bus when a system is installed with only AVR's was considered in [4]. Only CP type of representation was taken into account for both load flow and linearization to portray dynamic stability phenomenon in the above aforementioned reference. The concepts of Hopf bifurcations to an IEEE first benchmark model having generator of model 2.2 with flux linkages as state variables in the presence of Static Synchronous Compensator was applied by [5]. Control designs for power electronics dominated power systems for assessing small signal stability criteria was given by [6].

A South East Brazilian system was taken to apply the bifurcation concepts on parametrized Differential Algebraic Equations (DAE's) which have load growth direction and loading parameter as arguments to assess the selection of buses for dynamic voltage monitoring was considered in [7]. Application of Hopf bifurcation on DC-DC converter feeding constant power load is given in [8]. The estimation of available transfer capacity in a two-area system using bifurcation tools by taking an elementary classical model for synchronous machine was dealt by [9]. To make things simple, the above reference didn't consider saliency to make the nonlinear time domain simulation easy together with modeling loads with constant impedance to further use Krons reduction for facilitating ease in obtaining overall linearized model. The concepts of normal form coefficients for power system dynamics and the applicability of center manifold theorem at Hopf bifurcation points was discussed by [10]. Based on the literature gathered above, the following objectives were proposed as there weren't considered in the above references.

FOREX Publication
Open Access | Rapid and quality publishing
International Journal of
Electrical and Electronics Research (IJEER)
Research Article | Volume 13, Issue 2 | Pages 193-198 | e-ISSN: 2347-470X

1. To explore the maximum loadability of loads 'A' and 'B' modelled by amalgamation of constant impedance (CZ), current (CI), power (CP) *i.e.* ZIP industrial load model with increased generation in Kundur two area system shown in Figure 1 without PSS via Hopf bifurcation. The works of [11] gave insights into small signal modelling for eigenvalue analysis in the presence of industrial loads but didn't take the Hopf bifurcation analysis.
2. To show the applicability of PSS in putting off the Hopf bifurcation limits to an extent greater than the value obtained in objective (1).
3. To evaluate the performance of PSS enabled AVR system by recording the waveform of deviation in rotor angle after giving 0.1 p.u. step disturbance to reference voltage of AVR (Vref) to validate the eigenvalue analysis results at nominal loading and stressed loading.
4. To see the improvement in damping ratio of critical modes and swing modes after placing PSS.

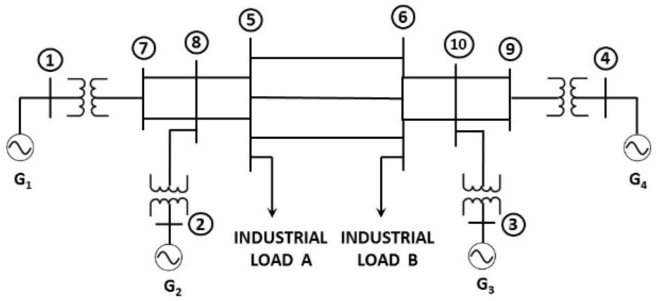

Figure 1. Kundur two area system one line diagram [SSRG]

2. MATERIALS AND METHODS

2.1 Power System Modelling

The synchronous machines are represented by detailed two axis model briefed in [3]. AVR has its associated static exciter represented with constant gain and time constant block. PSS having two stage lead lag blocks in cascade with washout block is provided for phase compensation which is shown in *figure 2*. Transmission circuits are modelled by nominal pi network and are assumed to be in quasi steady state thus making the use of static power flow equations expressed in polar coordinates to facilitate unburden for computations. Industrial loads are modelled by ZIP model as described by *equations 1-4* taken from [12].

$$P = P_0\left[\alpha_p + \beta_p\left(\frac{V}{V_0}\right) + \gamma_p\left(\frac{V}{V_0}\right)^2\right] \tag{1}$$

$$Q = Q_0\left[\alpha_q + \beta_q\left(\frac{V}{V_0}\right) + \gamma_q\left(\frac{V}{V_0}\right)^2\right] \tag{2}$$

$$\alpha_p + \beta_p + \gamma_p = 1 \tag{3}$$

$$\alpha_q + \beta_q + \gamma_q = 1 \tag{4}$$

In *equations (1) - (4)*, 'P', 'Q' represents real & reactive power consumed by load at voltage 'V'; 'P0', 'Q0' represent real and reactive power consumed at voltage 'V0'; αp, βp, γp & αq, βq, γq are the load composition coefficients corresponding to CP, CC & CZ models of *equations (1) & (2)* respectively. *Equations (3) & (4)* dictate that total composition is unity for both real and reactive parts of loads on right hand side of *equations (1) & (2)*. For industrial loads, the values of αp, βp, γp, αq, βq, γq are 1.41, -1.61, 1.21, 3.72, -7.08, 4.35 respectively.

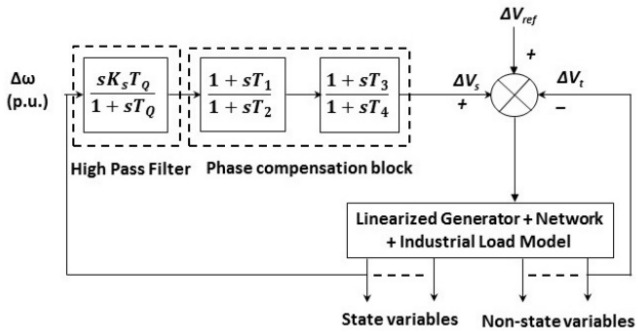

Figure 2. Power system stabilizer block diagram

Equations 1, 2 are linearized along with algebraic equations of transmission networks, DAE's of synchronous machines, static exciters and PSS at appropriate generator to get overall system matrix whose procedure is essayed in [3].

2.2 Concepts of Hopf bifurcation

The power system DAE's can be represented in the form of *Equations 5 and 6* where '*x*', '*y*', '*p*' represents the state, algebraic and control variables respectively.

$$\dot{x} = f\left(x, y, p\right) \tag{5}$$

$$0 = g\left(x, y, p\right) \tag{6}$$

Equations 7 and 8 are obtained after small perturbation of *equations 5 and 6*

$$\Delta\dot{x} = \left[\frac{\partial f}{\partial x}\right]^0 \Delta x + \left[\frac{\partial f}{\partial y}\right]^0 \Delta y \tag{7}$$

$$0 = \left[\frac{\partial g}{\partial x}\right]^0 \Delta x + \left[\frac{\partial g}{\partial y}\right]^0 \Delta y \tag{8}$$

Equations 9 and 10 are derived by proper matrix manipulation from *equations (7) & (8)* to assess parameter variation to assess system stability *via* Hopf bifurcation. The value 'p' can vary either as per both *equations 11 and 12* or *equation 11* only.

$$\Delta\dot{x} = \left[J_{SYS}\right]\Delta x \tag{9}$$

$$\left[J_{SYS}\right] = \left[\frac{\partial f}{\partial x}\right]^0 - \left[\frac{\partial f}{\partial y}\right]^0 \left[\left[\frac{\partial g}{\partial y}\right]^0\right]^{-1} \left[\frac{\partial g}{\partial x}\right]^0 \tag{10}$$

$$P_{L,i} = P_{L,i,0}\lambda_i \tag{11}$$

$$Q_{L,i} = Q_{L,i,0}\lambda_i \tag{12}$$

FOREX Publication
Open Access | Rapid and quality publishing
International Journal of
Electrical and Electronics Research (IJEER)
Research Article | Volume 13, Issue 2 | Pages 193-198 | e-ISSN: 2347-470X

where λ_i, $P_{L,I,0}$, $Q_{L,I,0}$ represents loading factor, nominal real and reactive power loading at i^{th} load bus respectively.

If all the latent roots of JSYS reside in the left half of the complex space, the system is small signal stable. For a given '*p*', even though *equation 6* is solvable, the latent roots of JSYS may surpass the imaginary axis to enter right half of S-plane thereby signalling dynamic instability. If only one conjugate pair of eigenvalues cross the imaginary axis while all the other values still don't cross to right half S-plane, then such a phenomenon is known as Hopf bifurcation. To apply the concepts of Hopf bifurcation to Kundur two area system, Cases A-G were created as defined below:

Cases A, B: Incremental rise in real part of load at 5th and 6th bus without PSS respectively.

Cases C, D: Incremental rise in real and imaginary part of load at 5th and 6th bus without PSS respectively.

Cases E, F: Incremental rise in real part of load at 5th and 6th bus with PSS respectively.

Cases G, H: Incremental rise in real and imaginary part of load at 5th and 6th bus with PSS respectively.

By increasing the generation in proportion to inertia constants of individual machines, compensation of load increase was done for power flows as suggested in [4].

2.3 Step by step explanation of the algorithm for eigenvalue & Hopf bifurcation analysis

1. Load flow & eigenvalue analysis: Treat loads as CP type to get steady-state values of variables for each step of loading parameter defined in cases A-H.

2. Perform axis-frame transformation to obtain machine variables. Linearize all the DAE's of system for forming system matrix without PSS for cases A-D.

3. For cases E-H, place PSS and obtain overall system matrix by linearizing all the DAE's. The details of optimal location of PSS in a system having loads modelled by ZIP based industrial model is furnished in [11.]. The PSS parameters were taken from [11].

4. For all cases, select a load bus and increase its loading by a suitable step size. Redo the power flows as given in [4] and once again repeat step-1 & 2. For cases E-H, perform step-3.

5. Identify critical mode that crosses the imaginary axis not *via* origin. Note the loading at which Hopf bifurcation occurs.

3. RESULTS AND DISCUSSIONS

3.1. Validation of the model developed & eigenvalue analysis

Coding in MATLAB 2020 environment for finding equilibrium points of network variables was done by Newton's method as power flow equations are non-linear and are expressed in polar coordinates by keeping the stopping criteria of real and reactive power mismatches to 10-12. The power flow data obtained in [13] was same as obtained in this manuscript and hence is not tabulated here. Generators G_1 and G_2 belong to area 1 and G_3, G4 belong to area 2 respectively.

To validate the system, the data given in [13] & [14] was taken and exact eigenvalues for CP, CC and CZ types of load representation cases was obtained for a zero mechanical damping by writing code in MATLAB environment. Now that the developed code exactly matched the results till forth decimal accuracy, composite load model for industrial loads was introduced instead of CP, CC & CZ models. To the best of author's knowledge, industrial load modeling for small signal stability assessment wasn't carried out by any of the researchers besides [11]. All the machine data presented in [13] was used except a minor modification of mechanical damping of 0.01 was considered for all the generators to avoid the occurrence of extra zero eigenvalue along with an additional eigenvalue that occurs due to lack of reference generator. For every power step defined in Cases A-H, Loads 'A' and 'B' are represented by constant power to get all unknown variables in power flow studies for initialization. The linearization program for expressing the overall state matrix in MATLAB considered ZIP load model taking industrial loads into account. The program was modified to exclude the zero eigenvalue by the procedure suggested in [13]. Using this method, the results of small signal analysis are tabulated in *table 1*. The damping ratio of swing mode 'a' is 0.1050 whose eigenvalue is given in first column of *table 1*. The damping ratio of swing mode '*b*' and inter-area mode is 0.1095 and 0.0081 respectively. The critical mode of interest is the inter-area mode and it can be observed that as with increased load and generation, this mode gets severely affected and transitions into the right half of S-plane as shown in *figure 3*.

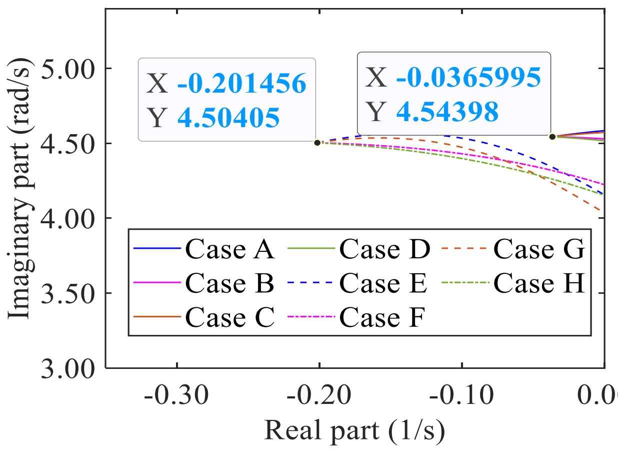

Figure 3. Locus of inter area mode for Cases A-H

As the damping ratio of inter-area mode is less than 3%, PSS was used to improve the same. It was suggested that the damping ratio of critical mode has to be at least 3% [15]. The values of PSS parameters at G4 were taken as T_1= 0.2473 s, T_2= 0.0218 s, T_3= 3 s, T_4= 5.4 s, T_Q= 10 s, Ks= 17.2079 to improve the damping ratio of inter-area mode to 0.0447 which is more than 3% [11]. But the placement has taxed the damping ratio of swing mode 'a' a little but significantly increased the damping ratio of swing mode 'b' to 0.3120 whose eigenvalues are shown in *table 1*. This is anticipated as the PSS is placed for G4 which is in the vicinity of *area 2*.

3.2. Time domain simulations in Δδ4 at nominal & stressed loadings

To see the performance of PSS, a 0.1 p.u. disturbance to ΔVref of AVR loop was initiated to look into small signal behavior of the various system variables. It can be seen in *figure 4* that without any PSS the complete damping of oscillations didn't occur in 40 s time frame. With PSS, the steady state deviation in delta *i.e.* Δδ4 is reached quickly. The system trajectory to show the locus of Δδ4 vs Δω4 (*i.e.* phase trajectories) after the disturbance initiation both with and without PSS cases are depicted in *figure 5*. Furthermore, the effect of PSS dynamics on the critical loading were demonstrated on Cases A-H and the results were obtained to be fruitful regarding the extension of Hopf bifurcation limit whose discussions are presented underneath.

Table 1. Eigenvalues at Nominal Loading

Eigenvalues	
Without PSS	**With PSS**
-24.3044 ± 28.3380i	-23.3240 ± 28.6866i
-25.0286 ± 13.5606i	-22.1820 ± 16.0529i
-0.7705 ± 7.2997i[a]	-0.7702 ± 7.2989i[a]
-0.7361 ± 6.6799i[b]	-1.9961 ± 6.0788i[b]
-0.0366 ± 4.5440i[c]	**-0.2015 ± 4.5041i[c]**
-39.9117, -39.3064	-57.0773, -39.7154
-11.7779, -11.2594	-16.2966, -11.4384
-4.5679, -4.4752	-4.5601, -4.4740
-4.2381, -4.1055	-4.2614, -4.1055
-0.0323	-0.0135, -28.3278
-	-0.1830 ± 0.0997i

a & b - Swing modes of area 1 & 2,
c- Inter area mode

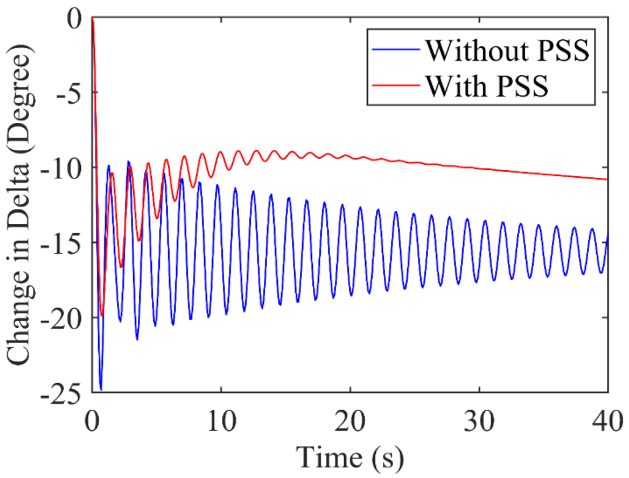

Figure 4. Curves showing variation of Δδ4 w.r.t time

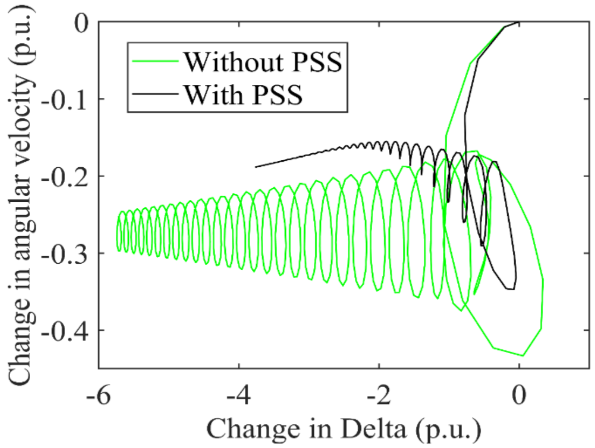

Figure 5. System trajectory showing Δδ4 vs Δω4

The eigenvalues corresponding to *sections 3.3-3.6* are presented in *table 2*.

3.3. Comparison of Case A and Case E

The critical swing mode 'c' is very close to Hopf bifurcation point for critical loading factor P5 of 13.04 p.u., without any PSS. The damping ratio of swing mode 'a' and 'b' are 0.0954 and 0.0966. With PSS device *i.e.* Case E, the load at the bus 5 can be increased till 21.5 p.u. which is more than the one obtained for Case A thus demonstrating the superiority of PSS placement. The damping ratio of swing mode 'b' is 0.2025 which is also greater than the one when compared to the similar variable for Case A, thus proving its efficacy at the Hopf bifurcation limit. The above result is anticipated as the PSS is placed in area 2 as seen in *table 2*. The imaginary part of inter-area mode for Case A is 4.5848i and for Case E, it is 4.1564i at the appropriate critical loadings. The unbounded wave forms of Δδ4 near the Hopf bifurcation point with and without PSS treatment is depicted in *figure 6* thus showcasing the validation of eigenvalue analysis.

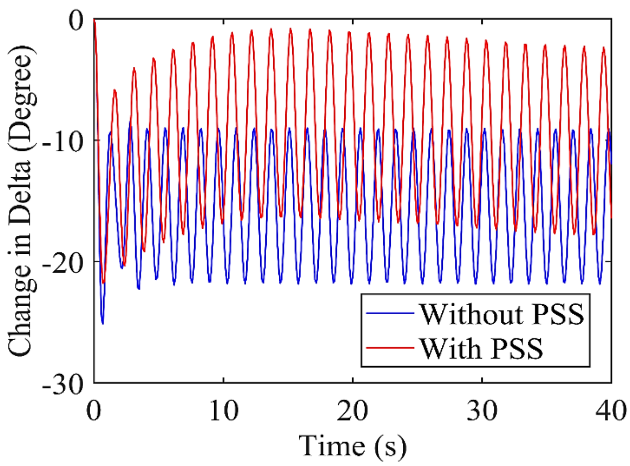

Figure 6. Variation of Δδ4 w.r.t time for Case A and E

3.4. Comparison of Case B and Case F

The critical swing mode 'c' is very close to Hopf bifurcation point for critical loading factor P6 of 17.04 p.u., without any

PSS. The damping ratios of swing mode ‘a’ and ‘b’ are 0.0962 and 0.0968 respectively. A critical loading of 22.18 p.u. at bus 6 was obtained with PSS device placement (Case F), which is more than the one obtained for Case B. The damping ratio of swing mode ‘b’ is 0.2402 which is higher when compared to Case B. The imaginary part of mode ‘c’ for case B is 4.5299i and for Case F is 4.2245i at equilibrium points very near to Hopf bifurcation limit. *Figure 7* shows the variation of Δδ4 w.r.t. time for Case B and F loadings.

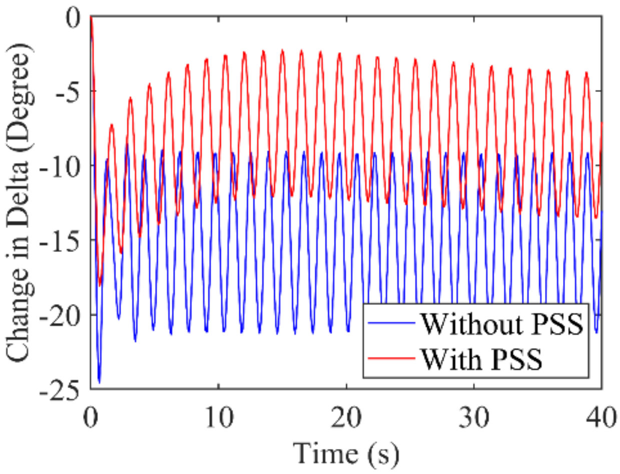

Figure 7. Variation of Δδ4 w.r.t time for Case B and F

3.5. Comparison of Case C and Case G

The critical swing mode ‘c’ is very close to Hopf bifurcation point for loading factor λ5 of 1.1355 without any PSS. The damping ratios of swing mode ‘a’ and ‘b’ are 0.0946 and 0.0954 respectively. A critical loading factor of 1.8265 at bus 5 was obtained with PSS device placement (Case G), which is more than the one obtained for Case C, thus demonstrating the usefulness of PSS presence. The other pros are the improvement in the damping ratio of mode ‘b’ i.e. 0.2010 over Case C swing mode damping ratio ‘b’. The imaginary part of mode ‘c’ for Case C is 4.5730i and for Case G it is 4.0348i at Hopf bifurcation limit. Figure 8 shows the variation of Δδ4 w.r.t time for Case C and G loadings depicting unbounded oscillations.

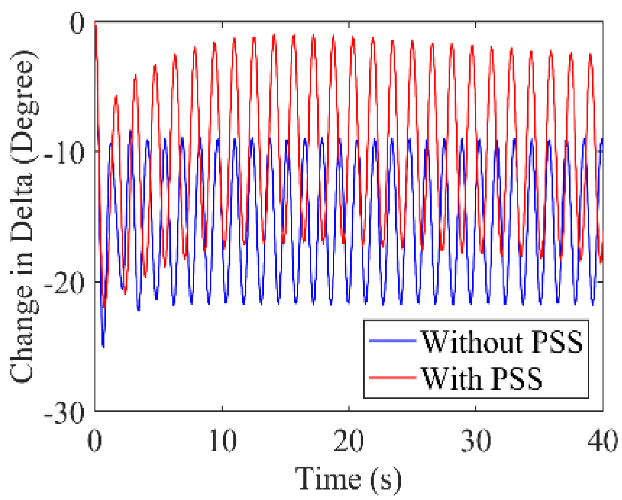

Figure 8. Variation of Δδ4 w.r.t. time for Case C and G

3.6. Comparison of Case D and Case H

The critical swing mode ‘c’ is very close to Hopf bifurcation point for loading factor λ6 of 1.0850 without any PSS. The damping ratios of swing mode ‘a’ and ‘b’ are 0.0958 and 0.0959 respectively. A critical loading factor of 1.3975 at bus 6 was obtained with PSS device placement (Case H), which is more than the one obtained for Case D. The other pros are the improvement in the damping ratio of mode ‘b’ i.e. 0.2304 over Case D swing mode damping ratio ‘b’. The imaginary part of mode ‘c’ for Case C is 4.5173i and for Case H it is 4.1541i near the Hopf bifurcation limit. *Figure 9* shows the variation of Δδ4 w.r.t time for Case D and H loadings.

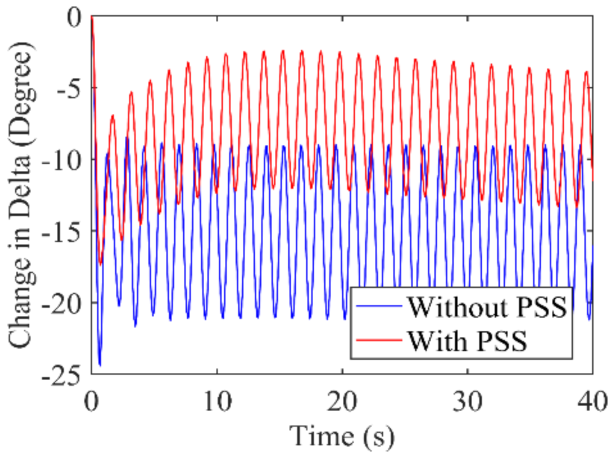

Figure 9. Variation of Δδ4 w.r.t time for Case D and H

Table 2. Eigenvalues with and without PSS at points near critical loading

Eigenvalues without PSS			
Case A, P_5 = 13.04 p.u.	**Case B, P_6 = 17.04 p.u.**	**Case C, λ_5 = 1.1355**	**Case D, λ_6 = 1.0850**
-24.2278 ± 29.2303i	-24.2332 ± 29.6209i	-24.2306 ± 29.4701i	-24.2353 ± 29.8806i
-25.0257 ± 13.5443i	-25.0277 ± 13.8097i	-25.0258 ± 13.7163i	-25.0282 ± 13.9527i
-0.7042 ± 7.3493i[a]	-0.7096 ± 7.3436i[a]	-0.6975 ± 7.3429i[a]	-0.7069 ± 7.3423i[a]
-0.6555 ± 6.7557i[b]	-0.6549 ± 6.7331i[b]	-0.6477 ± 6.7594i[b]	-0.6486 ± 6.7291i[b]
-0.0001 ± 4.5848i[c]	**-0.0002 ± 4.5299i[c]**	**-0.0001 ± 4.5730i[c]**	**-0.0000 ± 4.5173i[c]**
-39.9641, -39.3969	-39.8493, -39.2815	-39.8844, -39.3254	-39.7889, -39.2027
-11.7423, -11.2414	-11.8360, -11.3389	-11.8124, -11.3028	-11.9022, -11.3939
-4.6706, -4.5732	-4.6839, -4.5426	-4.6783, -4.5812	-4.6898, -4.5444
-4.3516, -4.1961	-4.3682, -4.2011	-4.3676, -4.2228	-4.3907, -4.2092
-0.0322	-0.0323	-0.0322	-0.0323
Eigenvalue with PSS			
Case E, P_5 = 21.50 p.u.	**Case F, P_6 = 22.18 p.u.**	**Case G, λ_5 = 1.8265**	**Case H, , λ_6 = 1.3975**
-22.1536 ± 51.0020i	-22.4040 ± 43.2550i	-20.3155 ± 73.7521i	-21.9144 ± 51.8256i

-22.2318 ± 19.5725i	-23.0920 ± 17.1987i	-22.2579 ± 20.8906i	-23.3651 ± 17.6029i
-21.8070 ± 3.1876i	-21.4114 ± 4.4644i	-21.6396 ± 4.2872i	-21.2084 ± 6.0070i
-0.3333 ± 7.5167i[a]	-0.4796 ± 7.4819i[a]	-0.3262 ± 7.4872i[a]	-0.4830 ± 7.4678i[a]
-1.3506 ± 6.5300i[b]	-1.5680 ± 6.3368i[b]	-1.3372 ± 6.5183i[b]	-1.4974 ± 6.3235i[b]
-0.0002 ± 4.1564i[c]	**-0.0003 ± 4.2245i[c]**	**-0.0000 ± 4.0348i[c]**	**-0.0005 ± 4.1541i[c]**
-57.6515, -38.8658	-57.4394, -39.2178	-57.5890, -38.1554	-57.2517, -39.0754
-12.4048, -0.0132	-12.0028, -0.0121	-13.0284, -0.0138	-12.1227, -0.0126
-5.2029 ± 0.2108i	-5.0929, -4.9657	-5.2071 ± 0.1948i	-5.1785, -4.9604
-0.1842 ± 0.1005i	-0.1907 ± 0.1089i	-0.1814 ± 0.0967i	-0.1878 ± 0.1053i
-5.1221, -4.7483	-4.7996, -4.5896	-5.1976, -4.7803	-4.8079, -4.5899

a) & b) Swing modes of area 1 & 2, c) Inter-area mode

4. CONCLUSIONS & LIMITATIONS OF THE STUDY

The improvement in the damping ratio of inter-area mode and the ability to extend the Hopf bifurcation taking both one and two parameter variation using PSS was demonstrated by DAE's of nonlinear power system modelled having ZIP industrial loads. Validation of PSS was also seen by taking a disturbance in reference voltage of AVR and was compared to the scenario where no PSS is present by time domain simulations of change in rotor angle $\Delta\delta 4$. However, to design PSS for real world applications, filters need to be designed in conjunction lead lag blocks considering system uncertainties. In future works, to address problems related to uncertainty in system parameters due to measurement errors, Kharitonov's theorems can be applied to achieve robust control in practical scenarios.

Acknowledgments: The first author thanks University Grants Commission (UGC), New Delhi, India for granting Junior Research Fellowship to do Ph.D. research work at Department of Electrical and Electronics Engineering, SVU College of Engineering, Sri Venkateswara University, Tirupati, India.

REFERENCES

[1] Devarapalli, R.; Sinha, N.K.; García Márquez F.P. A review on the computational methods of power system stabilizer for damping power network oscillations. Arch. Comput. Methods Eng, 2022, vol. 29, no. 6, pp. 3713-3739.

[2] Karimi, M.; Shahriari, A.; Aghamohammadi, M.R.; Marzooghi, H.; Terzija, V. Application of Newton-based load flow methods for determining steady-state condition of well and ill-conditioned power systems: A review. Int. J. Electr. Power Energy Syst., 2019, vol. 113, pp. 298-309.

[3] Dey, P.; Saha, A.; Bhattacharya, A.; Marungsri, B. Analysis of the effects of PSS and renewable integration to an Inter-Area Power Network to Improve Small Signal Stability. J. Electr. Eng. Technol., 2020, vol. 15, pp. 2057-2077.

[4] Shaik, G.A.; Aithepalli, L.D. Identification of Hopf bifurcation point using small signal stability analysis in a power system with increased load and generation. Proceedings of the Third International Conference on Advances in Electrical, Computing, Communication and Sustainable Technologies (ICAECT), Bhilai, India, 2023, pp. 1-4.

[5] Mala, R.C.; Prabhu, N.; Rao H.G. Hopf bifurcations of sub synchronous resonance in a hybrid series compensated system with SSSC-ES. Proceedings of the 2015 International Conference on Technological Advancements in Power and Energy (TAP Energy), pp. 65-72, 2015.

[6] Chen, Q.; Bu, S.; Chung, C.Y. Small-signal stability criteria in power electronics-dominated power systems: A comparative review. J. Mod. Power Syst. Clean Energy, 2023, vol. 12, pp. 1003-1018.

[7] Bento, M.E.; Ramos, R.A. An approach for monitoring and updating the load margin of power systems in dynamic security assessment. Electr. Power Syst. Res., 2021, vol. 198, pp.107365.

[8] Huang, L.; Y. Lu, Y.; Discrete modeling and period-adding bifurcation of DC–DC converter feeding constant power load. IEEE Access, 2021, vol. 9, pp. 52773-52783.

[9] Wei, J.; Li, G.; Zhou, M. Numerical bifurcation and its application in computation of available transfer capability. Appl. Math. Comput., 2015, vol. 252, pp. 568-574.

[10] Zhi, Y.; Wajid, H.; Venkatasubramanian, V.M.; Ji, W.; Panciatici, P.; Xavier, F.; Gilles, T. 2022. Computational methods for nonlinear analysis of Hopf bifurcations in power system models. Electr. Power Syst. Res., 2022, vol. 212, pp.108574.

[11] Shaik, G.A.; Aithepalli, L.D. Investigation of particle swarm optimization-based power system stabilizer on damping performance in two area system with voltage dependent load models. SSRG Int. J. Electr. Eng., 2025, vol. 12, no. 1, pp. 63-75.

[12] Kumar, A.; Jha, B.K.; Singh, D.; Misra, R.K. A new current injection-based power flow formulation. Electr. Power Components Syst, 2020, vol. 48, no. 3, pp. 268-280.

[13] Padiyar, K. R. Power System Dynamics Stability and Control, 2nd ed., BS Publications, Hyderabad, India 2008.

[14] Pai, M.A.; Sen Gupta D.P., Padiyar, K.R. Small Signal Analysis of Power Systems, Narosa Publishing House, New Delhi, 2004.

[15] Xi-Fan Wang; Yonghua Song.; Malcolm Irving. Modern Power Systems Analysis, Springer, New York, 2008.